Earth Syst. Sci. Data Discuss., https://doi.org/10.5194/essd-2018-22
Manuscript under review for journal Earth Syst. Sci. Data
Discussion started: 4 April 2018

North Atlantic subpolar gyre along predetermined ship tracks since 1993: a monthly dataset of surface temperature, salinity, and density.

Gilles Reverdin[1], Hedinn Valdimarsson[2], Gael Alory[3], Denis Diverres[4] , Francis Bringas[5], Gustavo Goni[5], Lars Heilmann[6], Leon Chafik[7], Tanguy Szekely[8], Andrew R. Friedman[9]

[1] LOCEAN, Sorbonne-Université, CNRS, IRD, MNHN, Paris, France

[2] Marine and Freshwater Research Institute, Reykjavik, Iceland

[3] LEGOS, Université de Toulouse, UPS, CNRS, IRD, CNES, Toulouse, France

[4] US IMAGO, IRD, Brest, France

[5] National Oceanic and Atmospheric Administration/Atlantic Oceanographic and Meteorological Laboratory, Miami, FL, USA

[6] Greenland Institute of natural resources, Nuuk, Greenland, DK

[7] Geophysical Institute, University of Bergen and Bjerknes Centre for Climate Research, Bergen, Norway

[8] IUEM, UMS3113, UBO-CNRS-RD, Plouzané, France

[9] School of Geosciences, University of Edinburgh, Edinburgh, Scotland, UK.

Earth Syst. Sci. Data Discuss., https://doi.org/10.5194/essd-2018-22
Manuscript under review for journal Earth Syst. Sci. Data
Discussion started: 4 April 2018

Earth System Science Data
Open Access
Discussions

Abstract

We present a binned product of sea surface temperature, sea surface salinity and sea surface density data in the North Atlantic subpolar gyre for the 1993-2017 that resolves seasonal variability along specific ship routes (https://dx.doi.org/10.6096/SSS-BIN-NASG). The characteristics of this product are described and validated through comparisons to other monthly products. Data presented in this work was collected in regions crossed by two predetermined ship transects, between Denmark and western Greenland (AX01) and between Iceland, Newfoundland, and the northeastern USA (AX02). The analysis and the strong correlation between successive seasons indicate that in large parts of the subpolar gyre, the binning approach is robust and resolves the seasonal time scales, in particular after 1997 and in regions away from the continental shelf. Prior to 2002, there was no winter sampling over the west Greenland shelf. Variability in sea surface salinity increases towards Newfoundland south of 54°N, as well as in the western Iceland Basin along 59°N. Variability in sea surface temperature presents less spatial structure with an increase westward and towards Newfoundland. The contribution of temperature variability to density dominates in the eastern part of the gyre, whereas the contribution of salinity variability dominates in the southwestern part along AX02.

Data availability

The gridded data set is freely available and accessible at https://dx.doi.org/10.6096/SSS-BIN-NASG

The XBT data collected along AX01 and AX02 is available at http://www.aoml.noaa.gov/phod/hdenxbt

Earth Syst. Sci. Data Discuss., https://doi.org/10.5194/essd-2018-22
Manuscript under review for journal Earth Syst. Sci. Data
Discussion started: 4 April 2018

1. Introduction

The North Atlantic Subpolar Gyre (NASG) has been extensively studied and observed during the last 25-years. This period presents the succession of a cold period in the early 1990s associated with strong North Atlantic Oscillation (NAO) forcing, a warmer period in 2000-2009, followed by a cooling (Robson et al., 2016), and strong NAO forcing in 2014 and 2015 (Josey et al., 2017). These conditions were associated with strong variability in intermediate water formed in the Labrador Sea, south-western Irminger Sea or South of Greenland, with strong formation years following strong atmospheric and NAO forcing years (Yashayaev and Loder, 2016; Fröb et al., 2015; de Jong et al., 2016, Piron et al., 2017). There has also been extensive variability in mode waters and their thickness in the northern or northeastern subpolar gyre, such as the Reykjanes mode water (Thierry et al, 2008) or the Rockall Trough mode water (Holliday et al., 2015). The changes in these subsurface water properties and distributions drive ocean circulation and in particular of the Atlantic Meridional Overturning Oscillation (AMOC) variability (Robson et al., 2016; Rahmstorf et al., 2015). The surface layer provides the link between the ocean interior and the atmosphere.

Surface variability in oceanic properties responds to atmospheric forcing and ocean circulation changes. In particular, NAO is known to strongly influence heat and freshwater fluxes in this region (Cayan, 1992; Hurrell et al., 2013; Bojariu and Reverdin, 2002) and thus sea surface temperature (SST) and sea surface salinity (SSS) (Josey and Marsh, 2005). Changes in freshwater fluxes from continental run-off and ice melt are also expected to change surface properties in the NASG (Böning et al., 2016). Net run-off from Greenland has considerably changed during the last decades (van der Broeke et al., 2016).The role of changes in ocean circulation have also been identified. For instance, the proportion of inflowing subtropical water was found to have increased in the 1995-2005 period compared to the previous two decades (Häkkinen et al., 2011; Häkkinen, 2013), followed by a net reduction of this input (Robson et al., 2016), which could have contributed to the more recent decadal cooling/freshening (see also Piecuch et al., 2017). A strong cold blob and anomalous cooling (and freshening) area has appeared in the

Earth Syst. Sci. Data Discuss., https://doi.org/10.5194/essd-2018-22
Manuscript under review for journal Earth Syst. Sci. Data
Discussion started: 4 April 2018

center of the NASG since the late-2000, and has also been linked indirectly to changes in the AMOC (Rahmstorf et al., 2015; Josey et al., 2017)

It has been speculated that the changes in atmospheric conditions, and of the resulting central gyre temperature and density associated with the strength of the gyre circulation are associated with zonal displacements of the subpolar front (Hatun et al., 2005; Sarafonov, 2009). This has been disputed (Foukal and Lozier, 2017), and has not been clearly identified in subsets of in situ current measurements along 59°N in two multi-year periods (Rossby et al., 2017), although recent analysis of altimetric sea level data also support an eastward displacement of the subpolar front during the recent period of strong atmospheric forcing (Zunino et al., 2017; their Fig. 8). The strong changes in thermocline and water masses associated with the fronts have been used by Stendardo et al (2017) to reconstruct surface temperature and salinity based on satellite altimetry data, which also suggests displacements of the subpolar front as a result of NAO forcing. However, this method does not work in the interior of the NASG.

Here, we present an effort to construct monthly time series of temperature (T), salinity (S) and density along tracks in the interior of the gyre. The data and methods used are first described in section 2, then the time series are presented in section 3. Basic characteristics are provided: interannual standard deviations and an EOF analysis of interannual variability. The characteristics of the data validation are presented in the appendices.

2. Data and Methods

2.1 Data

A large part of the data presented here are from SBE21 and SBE45 thermosalinographs (TSG) installed on ships running along the AX01 transect between Denmark and western Greenland and along the AX02 transect between Iceland, Newfoundland and the north-eastern USA (Fig. 1). Along AX01, TSG data were collected on M/V Nuka Arctica between July 1997-2017 (with intake temperature in 2005-2017). Along AX02, TSG data

Earth Syst. Sci. Data Discuss., https://doi.org/10.5194/essd-2018-22
Manuscript under review for journal Earth Syst. Sci. Data
Discussion started: 4 April 2018

are available between April 1994 and December 2007 and between March 2011 and March 2016 (with intake temperature during April 1994-1996).

The first installation on Nuka Arctica was done on a pumped water circuit in the bow thruster room of the ship, with little warming, but frequent interruptions during and after bad weather. In 2006, it was moved to the engine room at approximately mid-ship, roughly 5-m below the water line. During some winters (January-March 1997-2002) there were no cruises on this ship. The most common route crosses the North Atlantic subpolar gyre along 59°-59.5°N (B-AX01), but the ship has often taken a different route, in particular further north (N-AX01) (see e.g. Chafik et al., 2014, their Fig. 1). Along west Greenland, at least north of 62°N, the route is fairly repeated between transects and often runs in mid-shelf between ports-of-call, very often up to southern Disko Bay (G-AX01), with a few crossings in summer further north to Thule in northwest Greenland.

Along AX02, a succession of ships has been used, with different installations usually in the engine room at mid-ship, between 4 and 7 m below the water line. The route taken by these vessels is often roughly straight between southeastern Newfoundland and the western tip of the Reykjanes peninsula (Fig. 1, what we will refer as the standard route B-AX02), but with some deviations depending on sea ice or weather conditions. Due to seasonal sea ice, in particular, there were no standard TSG data on the route north-east of Newfoundland on shelf and slope in February-April 1994-1995 and 2014-2016.

The validation and correction of the TSG salinity data is mostly based on comparison with water samples collected from a water intake at the TSG (AX01 and AX02) and using nearby upper level of Argo float data (primarily for AX02) (Alory et al., 2015). On AX02, adjusting T from the TSG to near-surface ocean temperature was done when no intake measurements were available, largely based on comparison with T from Expandable bathythermograph (XBT) observations at 5-7 m. XBT observations along these two transects were started in 2000 (AX01) and 1993 (AX02) and have produced approximately 4,000 temperature profiles available for these comparisons. In addition T from the TSG on Nuka Arctica (AX01) were also used to adjust T along AX02 where

Earth Syst. Sci. Data Discuss., https://doi.org/10.5194/essd-2018-22
Manuscript under review for journal Earth Syst. Sci. Data
Discussion started: 4 April 2018

Open Access Earth System Science Data Discussions

there were crossovers of the AX01 and AX02 ships route. Validation of T and S data from the thermosalinographs is discussed further in App. A. For AX02, additional T and S data originate from seasonal surface sampling, in particular in July1993, January and April 1994, in 1995, and in 2007-2017. TSG data from several research cruises were also included. Upper-level data (near 5-7 m) of profiles from Argo, earlier PALACE floats (since 1996) and from CTD casts were also considered, as well as data from drifters equipped to measure precise temperature and salinity.

2.2 Methods

We construct monthly binned T, S, and density time series starting in mid-1993 along two standard sections intersecting near 59.5°N/32°W: B-AX01 between the North Sea and South Greenland and B-AX02 between Iceland and southern Newfoundland (Fig. 1). The B-AX01 section extends from the south-east of Cape Farewell (excluding the shelf or its vicinity) to the northwestern North Sea north-east of Scotland over the shelf. A separate binning G-AX01 is done on the Greenland shelf between southern Disko Bay (near 68.2°N/54°W) and northwest of Cape Farewell, but only since July 1996 (with no data north of 64.5°N in 1996-1997). We also binned data on an alternate route often used by Nuka Arctica across the Irminger Sea and Iceland Basin (N-AX01), to the north of B-AX01. For B-AX02, we include two bins over the Newfoundland shelf and two bins further to the north-east over the continental slope, followed by more regular bins along the standard section.

First, a gridded seasonal cycle is subtracted from the data to create anomalies that are then grouped in the bins on a monthly time scale. The average seasonal cycle is based on 120-year of data in the NASG (Friedman et al., 2017), and is on a 0.5° x 1° latitude x longitude grid. After creating the time series, the average seasonal cycle is modified and adjusted over the time series length to bring it back to no average anomalies. The actual average salinity is also provided, by adding this average seasonal cycle. Time series along B-AX01 contain some long-lasting data gaps until late 1997 that were filled with data along 58°N or 60°N, therefore larger errors attributed. Along, G-AX01, there are no winter data (January- March) in 1997-2002. Time series along B-AX02 start in July 1993

Earth Syst. Sci. Data Discuss., https://doi.org/10.5194/essd-2018-22
Manuscript under review for journal Earth Syst. Sci. Data
Discussion started: 4 April 2018

with few gaps longer than three months, the longest being associated to winters with ice presence over the Newfoundland shelf or slope. The time series are then smoothed by a 1-2-1 running-mean over successive months. Before performing an empirical orthogonal function analysis (EOF), gaps in the time series are filled by first linearly interpolating from neighboring spatial bins, and then in time from neighboring time steps. They are then normalized to unit variance. Comparison of this gridded product against other gridded products is provided in App. B.

3. Results

3.1 variability along AX01 and AX02

The Hovmøller diagram of seasonal salinity anomalies are presented on Fig. 2. A rather similar variability is portrayed where the two sections B-AX01 and B-AX02 intersect, although clearly B-AX01 indicates a strong longitude dependence of the signals portrayed just to the east of the intersection of B-AX02.

The B-AX02 salinity plot (Fig. 2, top right) suggests large spatial variations characterized by interannual to decadal variability. On the shelf and slope regions, in particular near Newfoundland, there seems to be more short-term variability. However, in these regions, error estimates are also larger, to some extent as a result of insufficient sampling, as well as due to unresolved high-frequency variability. This results in weak correlation of S anomalies between successive seasons (three months apart), although there is a tendency for negative low frequency anomalies until 2000 and since 2010. Correlation in other regions of AX02 between successive seasons is larger (correlation coefficient at least 0.6), indicating a dominance of interannual and lower frequency variability over intra-annual variability. There is less spatial variability along B-AX01 (Fig. 2, top left). There is a tendency for differences across the Reykjanes ridge, such as in 1994 or 2015-2017, with large negative anomalies in the western Iceland Basin. Variability on European shelves tend also to be different. On B-AX01, correlation is also large between successive seasons, with an exception in the last 200 km from the shelf break off southern Greenland. There, however, the TSG transects do not resolve well enough the spatial and temporal variability.

Temperature anomalies (Fig. 2, middle panel) tend not to be correlated with the salinity ones, although there is some suggestion that the decadal variability is correlated (except on the shelves). This is seen here as the negative SST anomalies near the beginning and end of the time series with warmer temperatures in the 2000-2009 period, roughly corresponding to SSS variability of the same sign. Variability is slightly larger along B-AX02, as expected from the known westward increase in SST variability portrayed for example in the Hadley Centre SST data set (HADSST3). Altogether there is not a large spatial variability in the temperature signals along these transects, at least on seasonal or longer time scales, except for some differences on the southern part of B-AX02 compared to other regions.

Density anomalies (Fig.2, lower panel) are a result of both temperature and salinity anomalies. Except in the southern part of B-AX02 (south of 54°N), temperature variability tends to have a larger contribution than salinity variability to density (in particular east of the Reykjanes Ride or north of 60°N). Thus, as for T, density anomalies along B-AX01 tend to present small longitudinal variations, with in particular highest positive density anomalies in the first few years and in mid-2014 to early-2016. Since early 2016, negative density anomalies are confined east of the Reykjanes Ridge. Along B-AX02, there is a larger contrast, with a transition near 52-54°N, with the density anomalies looking more like S south of it and more like T north of it. The correlation between density anomalies in successive seasons is also smaller for surface density than for T and S.

To a large extent, section N-AX01 (Fig. 3) presents variability that is coherent with what is seen on B-AX01 along 59°N (Fig. 2). However, whereas in the Iceland Basin near 10-18°W along N-AX01, one also finds the freshening happening by mid-2015, further west (and closer to Iceland) as well as in the northeastern Irminger Sea east of 35°W, the freshening happens later in 2016 and 2017 (with some suggestion of a weaker winter signal). This did not show up further south along 59°N in the eastern Irminger Sea away from the Reykjanes Ridge until late 2017 (Fig. 2). Along N-AX01, at 20°W, very close to

Earth Syst. Sci. Data Discuss., https://doi.org/10.5194/essd-2018-22
Manuscript under review for journal Earth Syst. Sci. Data
Discussion started: 4 April 2018

southern Iceland, there are also isolated patches of larger anomalies, possibly related to local freshwater inputs from Iceland. To the east of the section, the last bin near the Shetlands Islands portrays a variability often very close to what is found further west in the deeper Ocean, whereas the two easternmost bins of the section along 59°N on the shelf (northwest and northeast of Scotland) seem to present a different variability.

Finally, variability on the west Greenland southwestern shelf (Fig. 3) is rather different for S than to the east in the Irminger Sea along B-AX01 or N-AX01. Except for the most southern box to the west of Cape Farewell, variability in S is rather coherent meridionally. For example, negative anomalies are observed in 2000, from mid-2006 to early 2009, and even more in 2010-2013 with a peak in the second half of 2012, and positive anomalies in 2015-2017. The extreme negative S values in late 2012 are consistent with the outstanding Greenland sheet melt that occurred that year (van der Broeke et al., 2016; Fettweis et al., 2017). On the other hand, other years with very large southern Greenland ice sheet melt (1995, 2002, 2005-2007, 2010, 2011) do not show as well in surface salinity. Temperature variability tends to be also of the same sign along the section, but with some notable exceptions. For instance, negative T anomalies are found in 2015-2017 north of 65°N, and not further south.

3.2 Interannual RMS variability

For each month of the calendar year, we evaluate the interannual RMS variability for each spatial bin. This gives us an estimate of the seasonal cycle of the interannual RMS variability (Fig. 4). For S (Fig. 4, top panels), large RMS values are found on the southern part of B-AX02 with a large decrease between 52°N and 54°N (52 and 53°N in winter). Near 55°N, there is minimum variability during winter-spring, then increases again near 57-59°N, followed by a strong decrease towards Iceland. RMS variability in S presents a seasonal cycle with a spring minimum over the Newfoundland shelf, which is less noticeable along the continental slope. Further offshore and until 54°N, there is a minimum variability in spring (and maximum during late summer/autumn). North of 54°N, there is a winter to late winter minimum although very weak near 56-59°N. This winter to early spring minimum is also very prominent along N-AX01, except in western

Earth Syst. Sci. Data Discuss., https://doi.org/10.5194/essd-2018-22
Manuscript under review for journal Earth Syst. Sci. Data
Discussion started: 4 April 2018

Irminger Sea, close to the Greenland shelves (not shown). Along B-AX01 at 59°N for S, the maximum RMS variability is found in the western Iceland Basin (20-30°W), then less further east (as well as in the Irminger Sea). There are also larger RMS east of 10°W along shelves/north-western North Sea (and last eastern box of N-AX01 near the Shetlands). There is not much seasonal variability in RMS along 59°N, although with weaker RMS in winter-early spring in the Irminger Sea.

For T (Fig. 4, middle panels), larger variability is found south of 54°N towards Newfoundland (except on the shelf, where winter SST variability is lower). Along 59°N, larger variability is found in the western Irminger Sea and eastern Iceland Basin. There is a seasonal modulation of RMS values with larger values in June-July north of 54°N along B-AX02 and along 59°N. In the western Irminger Sea or south of 54°N closer to Newfoundland, maximum RMS is shifted later in July to early autumn.

The surface density RMS seasonal cycle (Fig. 4, lower panels) is a mix of what is seen on temperature and salinity. Along B-AX01 and N-AX01, density variations are dominated by temperature variations, except west of 40°W along B-AX01 and close to Iceland, where S and T have comparable contributions. Along B-AX02, south of 54°N, salinity contributes more to density variability than temperature, whereas further north, the two contributions are of a similar magnitude.

3.2 EOF analysis

When performing an EOF analysis on S, on B-AX01 and B-AX02 together, little seasonal dependence is observed in the first two components**:** similar time series are almost found when performing the EOF analysis on the whole time series or on low passed filtered time series for different seasons (not shown). The associated principal components are very similar for the two tracks, thus we jointly analyzed the two gridded data sets after low-pass filtering by the 15-month running mean filter (Fig. 4). The principal components associated with EOF1 and EOF2 both present a large variability at periods of 5 years or more. PC1 largest negative anomalies are in 1994-95 and in 2016-2017, and largest positive values in 2004 and 2009, whereas PC2 largest negative values

Earth Syst. Sci. Data Discuss., https://doi.org/10.5194/essd-2018-22
Manuscript under review for journal Earth Syst. Sci. Data
Discussion started: 4 April 2018

are in 2015, but with an apparent trend superimposed. PC1 resembles the sea surface height variability in the northern North Atlantic and hence gyre variability (Chafik et al., 2018).

EOF1 has large positive values across the two sections, except in the far west of AX01 (close to the east Greenland Current), and on the Labrador shelf. EOF2, which overall explains only 14% of the variance, has positive values both in the Labrador Sea (B-AX02 south of 53°N) and in the western Iceland Basin (27-17°W) along B-AX01 (to a smaller scale), with negative values in the Irminger Sea along AX01 peaking near 40°W. Maximum values (where it is positive) never explain more than 50% of the local variance. EOF3 (10% of the variance) has large values only over the Labrador shelf and slightly north of it until 55°N along B-AX02, and seems to correspond to higher frequency variability.

Data availability

The gridded data set is freely available and accessible at https://dx.doi.org/10.6096/SSS-BIN-NASG

The XBT data collected along AX01 and AX02 is available at http://www.aoml.noaa.gov/phod/hdenxbt

4. Conclusion

The validated data presented here are able to characterize the seasonal variability of surface temperature and salinity along two transects crossing the North Atlantic subpolar gyre (along 59°N and from south-west Iceland to south-east Newfoundland) from July 1993 to December 2017. The time series presented here describe the interannual variability at seasonal resolution over this 21 to 25-year period except for some winter gaps over the Newfoundland shelf and along west Greenland, as well as until 1996 in the Iceland Basin along 59°N, and until mid-1997 along parts of west Greenland. To describe this variability these time series are better than current SST or SSS ocean data gridded analyses such as those provided in EN4 or CORA, in particular before the Argo period. These time series provide added information, in particular on the shelves and continental slope regions that is not available from Argo float data, despite Argo reaching nominal

Earth Syst. Sci. Data Discuss., https://doi.org/10.5194/essd-2018-22
Manuscript under review for journal Earth Syst. Sci. Data
Discussion started: 4 April 2018

density since the early 2000s. Also, they are complementary to indirect analyses of the variability based largely on satellite altimetry (Stendardo et al., 2016), which only work as long as a strong relationship between dynamic height, sea level and surface T and S exist, such as near fronts in the open ocean (Dong et al., 2015). This excludes most of the area investigated here.

In the interior of the subpolar gyre, the time series can be used to precisely monitor the arrival of very large freshwater salinity anomalies in recent years, and to characterize how they relate or not with temperature anomalies. They also suggest similarities with an earlier event in 1994-1996, which is unfortunately not as well sampled overall (Reverdin et al., 2002). The salinity time series are rather different on the shelves sampled here, in particular west of Greenland and near Newfoundland. This is expected, because of the different water masses with a large proportion of water advected from the Arctic or influenced by continental inputs. Sampling with the ships of opportunity is not always sufficient in these areas, due to the presence of seasonal sea ice, and would need to be complemented by other observational platforms.

In some areas, such as on the shelves or south of 54°N along B-AX02, there is a seasonal modulation of surface salinity variability. In most areas, salinity variability tend to be largest in summer or early autumn, although there are areas, such as along 59°N, with a weak seasonal cycle of this variability. Further interpretation of these data would require at least contemporary information on air-sea fluxes (heat, fresh water), mixed layer depth, and ocean circulation.

Results and data presented here highlight the importance of repeated ocean observations from volunteer ships, and the value of complementary data to better assess and monitor the state of the ocean and its variability from seasonal to interannual time scales.

Appendix A: Validation of TSG data

TSG observations from M/V Nuka Arctica form the core of the B-AX01, N-AX01 and G-AX01 are available since 1997. The salinity values were validated and adjusted using mostly surface water samples following Alory et al. (2015). An intake temperature measurement was used since late 2004 to adjust the temperature measurements reported by the TSG. Before that, ad hoc adjustment was made on Nuka Arctica TSG temperature based on comparison with nearby data, but showing often very small differences, of less than 0.1°C.

We checked the consistency of these T-S data of Nuka Arctica with other upper ocean data. The TSG temperature and salinity data do not present significant biases with the upper level of Argo profiles, close to 5-8 m depth. The average differences (TSG-Argo) in T of 0.03°C and in S of 0.01 psu are compatible with 0 at the 95% level (based on 226 profiles within 50 km and 5 days of ship's track, accepting differences of 1°C and of 0.2 psu, which removes 11% of outliers).

The 'adjusted' temperature reported by the TSG was also compared with the temperature of the XBTs launched usually every three months from the *Nuka Arctica* since 2001 (Rossby et al., 2017). The comparison was done with XBT temperature at 7-m depth. We first average the comparisons over individual transects and estimate a mean and RMS difference. Then we average these transect summaries. When removing 5 transects for which there is too large a scatter in the individual matches (RMS difference larger than 0.2°C), the average temperature difference for 40 transects is -0.056°C with an RMS difference between individual transect summaries of 0.075°C (if individual transects were independent and in a Gaussian distribution, this would result in a 95% percentile range between -0.032 and -0.080°C). This average difference fits with the expected near surface temperature warm bias of XBTs for those years (Reverdin et al., 2009). The five occurrences with larger scatter fall in two categories: two in early June in the eastern part of the section with weak wind and a very likely stratification near the surface, resulting in T from the TSG higher than T from the XBT profiles at 7m, and three where the flow rate was very weak (in 2001-2003). With the TSG placed in the bowhead of the ship until 2005, it is unlikely that T measured during those transects would present large biases with respect to outside SST, although clearly there is a time lag and time integration of the ocean temperature in those records. Because data at large spatial scales seemed

Earth Syst. Sci. Data Discuss., https://doi.org/10.5194/essd-2018-22
Manuscript under review for journal Earth Syst. Sci. Data
Discussion started: 4 April 2018

reasonable during these weak-flow instances, including the 5 events does not change significantly the average bias. Thus, we retained these data in the data set, despite the likely time delay. In summary, although there can be errors on individual transects, the comparisons suggest high consistency between TSG data and other validated data a few meters below the surface.

We carried a similar comparison for TSG data AX02 data since 1994, but although average results are similar, scatter is larger. The comparisons are also more difficult to interpret, because of many changes in how and where the TSGs were installed on different ships during the 1994-2016 period, frequent insufficient flow through the instrument, and also because XBT and Argo data were used to adjust the TSG temperatures when there was no intake temperature measurements. Notice also that for 6 crossings (in July 1993, January and April 1994, as well as in 2016-2017), temperature was measured by the bucket method, taking care of leaving the bucket long enough in the sea and measuring T quickly (within 30 seconds) after retrieving the bucket. The data were compared for two crossings with intake temperature measurements, suggesting small negative biases (at most -0.1°C), except during high wind conditions, which were not frequent.

Appendix B: comparison with ENACT, CORA and Armor3D gridded products

Mapped analysis products of the hydrographic data sets EN4 and CORA6.1 are based on objective mapping (Good et al., 2013 for EN4 and Cabanes et al., 2013, Gaillard et al., 2013 for CORA/ISAS), and contain a level near the surface which is used here. Mapped products from Armor3D are largely based on altimetric sea level data with T and S adjusted to in situ T and S profiles (Guinehut et al., 2012).

We compare the binned (B-AX01) monthly time series (59-60°N) (left panels of fig. 4) to interpolated EN4, CORA6.1 and Armor3D products at the same sites and with additional 1-2-1 smoothing applied over successive months (EN4-AX01, CORA-AX01, Armor3D-AX01) (June 1993 to December 2015). The results are summarized by presenting longitude sections of correlation and RMS variability (Fig. B1). For S, there is little correlation in SSS with EN4, except in the western Iceland Basin, and RMS variability is much higher in EN4 surface fields (often by a factor of 2). Amplitudes are closer in CORA-AX01 and Armor3D-AX01, although there are smaller than those observed in the eastern Irminger Sea, and correlation is high except near the slopes. Interestingly, when averaging vertically EN4 salinity over the 0-500m layer, correlation with B-AX01 strongly increases everywhere (with coefficients often larger than 0.6), and becomes significant and comparable to what is found for CORA-AX01 or Armor3D-AX01, except in the central and western parts of the Irminger Sea. Although this is a region where it is known that surface low frequency variability tends to be correlated at depth (Reverdin et al., 2018 or the old one?), one expects a decrease of correlation between the surface and greater depths. The better correlation with vertically integrated quantities than with analysis at the same (5 m) level in EN4 suggests that 'noisy' or 'erroneous' data are not properly filtered in the EN4 surface analysis. It is also found that CORA analyses are more correlated vertically that EN4, which points in the same direction. To a large extent, CORA and EN4 products rely on the same data, largely to Argo (and earlier PALACE) floats as well as research cruise CTD data, whereas B-AX01 strongly relies on TSG data (to a large extent from Nuka Arctica). These mapped products differ in how they are produced. EN4 will tend to stick more to local data, whereas CORA analysis scheme is a classical objective mapping of deviations from a guess field. Thus, it will damp variability when there is not enough data within the radius of integration (Gaillard et al., 2009). This is likely to have often been the case before the Argo float deployments in 2001-2002. Thus, CORA will underestimate the variability, but be less noisy. The lack of data probably also explains the absence in this product of the low salinity signals in 1993-1995.

For SST, the correlation of B-AX01 with all the gridded products along this zonal section is quite large (larger than 0.80 everywhere, albeit a little smaller for Armor3D) with RMS variability of the same magnitude to the one in B-AX01 in the different products (although slightly smaller in CORA). The data coverage (XBTs in addition to Argo, PALACE and CTD casts) is often quite good, with largest differences in 1993-1996 when data coverage is weaker. Despite possible near surface stratification, the large similarity

Earth Syst. Sci. Data Discuss., https://doi.org/10.5194/essd-2018-22
Manuscript under review for journal Earth Syst. Sci. Data
Discussion started: 4 April 2018

in T between B-AX01 and EN4 suggests that the different temperature data sets are consistent. The correlation with vertically integrated temperature is smaller than at the surface and rather similar in the two products, again pointing to rather well data-constrained analyses.

The comparison of TSG data with Argo profile data (App. A) gives confidence in S from Nuka Arctica and thus in B-AX01 time series. Thus, the large difference in S between EN4 and B-AX01 is indicative of large seasonal noise in EN4 surface salinity, maybe resulting from the insufficient sampling of meso-scale, short-term variability, in particular from Argo and other (earlier) profiling salinity floats. In the western and central Irminger Sea, the objective mapping technique used in EN4 could also spread an influence of distant data of the cold and fresh water of the east Greenland shelf and slope, which have very different values.

Author contribution

GR has contributed to the data validation and data compilation along the two ship of opportunity lines (AX01 and AX02) since the project was initiated in 1993. HV has provided support in Iceland and contributed to the scientific discussion on the data compilation. GA has been in charge of AX02 data correction and validation. DD has installed the TSG on M/V Nuka Arctica in 1997 and monitored the data since then. FB and GG at NOAA/AOML have supported the TSG and XBT operations for many years on AX02. LC has contributed to the comparison of the gridded products to EN4, and TS has contributed to the comparison of the gridded product with CORA. LH has been the contact for Nuka Arctica in Nuuk (Greenland) and analyzed a large part of the water samples used for the data calibration of AX01.

We have not identified any conflict of interest.

Acknowledgements

This is a contribution to the French SSS observation service, which is supported by French agencies INSU/CNRS, IRD, CNES and IPEV. We are very grateful to the crews of the different vessels on lines AX01 and AX02 from which the salinity data have been collected, in particular under the EIMSKIP and Royal Arctic Line (RAL) managements. We acknowledge the strong support to this operation by Lars Heilman in Nuuk, Magnus Danielsen in Reykjavik, Hans Magnussen in Aalborg, Denis Pierrot and Francis Bringas. NOAA/AOML and NOAA/CPO Ocean Observing and Monitoring Division have contributed by maintaining the TSGs along AX02 and providing XBTs on the different ships that have operated along the AX01 and AX02 transects. Coriolis contributed by providing XBTs to M/V Nuka Arctica and by supporting the production of the CORA dataset. ARMOR3D (G LOBAL_REP_PHY_001_021) products are freely available through the Copernicus Marine Environment Monitoring service.

Earth Syst. Sci. Data Discuss., https://doi.org/10.5194/essd-2018-22
Manuscript under review for journal Earth Syst. Sci. Data
Discussion started: 4 April 2018

References

Alory, G., T. Delcroix, T., Téchiné, P., Diverrès, D., Varillon, D., Cravatte, S., Gouriou, Y., Grelet, J., Jacquin, S., Kestenare, E., Maes, C., Morrow, R., Perrier, J., Reverdin, G., Roubaud, F.: The French contribution to the Violuntary Observing Ships Network of Sea Surface Salinity. Deep Sea Res. I, 105, 1-18, doi:10.1016/j.DSR.2015.08.005, 2015.

Bojariu, R., and Reverdin, G.: Large-scale variability modes of freshwater flux and precipitation over the Atlantic. Climate Dyn., 18, 369-381, 2002.

Böning, C. W., Behrens, E., Biastoch, A., Getzlaff, K., and Bamber, J. L.: Emerging Impact of Greenland Meltwater on Deepwater Formation in the North Atlantic Ocean. Nature Geoscience. https://doi.org/10.1038/ngeo2740, 2016.

Cabanes,C., Grouazel, A., Von Schuckmann, K., Hamon, M., Turpin, V., Coatanoan, C., Paris, F., Guinehut, S., Boon, C., Ferry, N., De Boyer Montegut, C., Carval, T., Reverdin, G., Pouliquen, S., le Traon, P.-Y.: The CORA dataset: validation and diagnostics of in-situ ocean temperature and salinity measurements. Ocean Science, 9,1-18, 2013.

Cayan, D. R.: Latent and sensible heat flux anomalies over the northern oceans: driving the sea surface temperature. J. Phys. Oceanogr., 22, 859-881, 1992.

Chafik, L., Rossby, T., Schrum, C.: On the spatial structure and temporal variability of poleward transport between Scotland and Greenland. J. Geophys. Res., 119, 824-841. Doi:10.1002/2013JC009287, 2014.

De Jong, M. F., and de Steur, L.: Strong winter cooling over the Irminger Sea in winter 2014-2015, exceptional deep convection, and the emergence of anomalously low SST. Geophys. Res. Lett., 42, doi: 10.1002/2016GL069596, 2016.

Dong, S., Goni, G. and Bringas, F.:. Temporal variability of the South Atlantic Meridional Overturning Circulation between 20°S and 35°S. Geophys. Res. Lett., 42, 18, 7655-7662, doi:10.1002/2015GL065603, 2015.

Fettweis, X., Box, J. E., Agosta, C., Amory, C., Kittel, C., Lang, C., van As, D., Macguth, H., and Gallée, H.: Reconstructions of the 1900-2015 Greenland ice sheet surface mass balance using the regional climate MAR model. The Cryosphere, 11, 1015-1033, doi:10.5194/tc-11-1015-2017, 2017.

Foukal, N. P., and Lozier, M. S.: Assessing variability in the size and strength of the North Atlantic subpolar gyre. J. Geophys. Res.: Oceans, doi: 10.1002/2017JC012798, 2017.

Friedman, A.R., Reverdin, G., M. Khodri, M., and G. Gastineau, G.: A new record of Atlantic sea surface salinity from 1896 to 2013 reveals the signatures of climate variability and long-term trends. Geophys. Res. Lett., 44, 1866–1876, doi:10.1002/2017GL072582, 2017.

Fröb, F., Olsen, A., Vage, K., Moore, G. W., Yashayaev, I., Jeansson, E., and Rajasakaren, B.: Irminger Sea deep convection injects oxygen and anthropogenic carbon to the ocean interior. Nat. Commun., doi:1038/ncomms13244, 2016.

Gaillard, F., Autret, E., Thierry, V., Galaup, P., Coatanoan, C., Loubrieu, T.: Quality control of large Argo datasets, J. Atmos. and ocean. Tech., 26 , 337-351, 2009.

Good, S. A., Martin, M. J., and Rayner, N. A.: EN4: quality controlled ocean temperature and salinity profiles and monthly objective analyses with uncertainty estimates, J. Geophys. Res., 118, 6704-6716, 2013.

Earth Syst. Sci. Data Discuss., https://doi.org/10.5194/essd-2018-22
Manuscript under review for journal Earth Syst. Sci. Data
Discussion started: 4 April 2018

Guinehut, S., Dhomps, A. L., Larnicol, G., and Le Traon, P. Y.; High-resolution 3-D temperature and salinity fields derived from in situ and satellite observations. Ocean Sci., 8, 845-857, 2012, doi: 10.5194/os-8-845-2012.

Hatun, H., Sando, A. B. Drange, H., Hansen, B., and Valdimarsson, H.: Influence of the Atlantic subpolar gyre on the thermohaline circulation. Science, 309, 1841-1844, 2005.

Holliday, N. P., Cunningham, S. A., Johnson, C., Gary, S. F., Griffiths, C., Read, J. F., and Sherwin, T.: Multidecadal variability of potential temperature, salinity, and transport in the eastern subpolar North Atlantic. J. Geophys. Res., 5945-597, doi:10.1002/2015JC010762, 2015.

Hurrell, J. W., Kushnir, Y., Ottersen, G., and Visbeck, M.: An overview oft he North Atlantic Oscillation: climate significance and Environmental impact. Geophys. Monogr. Ser., published by A.G.U., doi:10.1029/134GM01, 2013.

Josey, S. et al.: The recent Atlantic cold anomaly: causes, consequences and related phenomena. Ann. Rev. Mar. Sci., 2017.

Kolodziejczyk N., Prigent-Mazella A., Gaillard, F.: ISAS-15 temperature and salinity gridded fields. SEANOE. http://doi.org/10.17882/52367, 2017.

Piecuch, C., Ponte, R. M., Little, C. M., Buckley, M. W., and Fukumori, I.: Mechanisms underlying recent changes in subpolar North Atlantic Ocean heat content, J. Geophys. Res., 122, 7181-7197, doi:10.1002/2017JC012845, 2017.

Piron, A., Thierry, V., Mercier, H., and Caniaux, G.: Gyre-scale deep convection in the subpolar North Atlantic Ocean during winter 2014–2015, Geophys. Res. Lett., 44, 1439–1447, doi:10.1002/2016GL071895, 2017.

Rahmstorf, S., Box, J. E., Feulner, G., Mann, M. E., Robinson, A., Rutherford, S., and Schaffernicht, E. J.: Exceptional twentieth-century slowdown in Atlantic Ocean overturning circulation. Nature Climate Change, 5(5), 475–480, 2015. http://doi.org/10.1038/nclimate2554.

Reverdin, G., Durand, F., Mortensen, J., Schott, F., Valdimarsson, H., Zenk, W.: Recent changes in the surface salinity of the North Atlantic subpolar gyre. J. Geophys. Res., 107, C12, 8010, doi:10.1029/2001JC001010, 2002.

Robson, J., Ortega, P., and Sutton, R.: A reversal of climate trends in the North Atlantic since 2005. Nature Geosci., 9, 513-517, doi:10.1038/ngeo2727, 2016.

Rossby, T., Reverdin, G., Chafik, L., and Soiland, H.: A direct estimate of poleward volume, heat, and freshwater fluxes at 59.5°N between Greenland and Scotland, J. Geophys. Res., doi:10.1002/2017JC012835, 2017.

Sarafonov, A.: On the effect of the North Atlantic Oscillation on temperature and salinity of the subpolar North Atlantic intermediate and deep waters. Ices J. of Mar. Sci.: Journal du Conseil, 66, 1448-1454, 2009.

Skliris, N., Marsh, R., Josey, S. A., Good, S. A., Liu, C., and Allan, R. P.: Salinity changes in the World Ocean since 1950 in relation to changing surface freshwater fluxes. Climate Dynamics, 43(3-4), 709–736. http://doi.org/10.1007/s00382-014-2131-7, 2014.

Stendardo, L., Rhein, M., and Hollmann, R.: A high resolution salinity time series 1993-2012 in the North Atlantic from Argo and altimeter data. J. Geophys. Res., doi:10.1002/2015JC011439, 2016.

Thierry, V, de Boisséson, E., and H. Mercier, H.: Interannual variability of the subpolar mode water properties over the Reykjanes Ridge. J. Geophys. Res., doi:10.1029/2007JC004443, 2008.

Van der Broeke, M., Enderli, E., Howat, I., Munneke, P. K., Noël, B., van de Berg, W., van Meijgaard, E., and Wouters, B.: On the recent contributions of the Greenland ice sheet to sea level change. The Cryosphere Discuss., doi: 10.5194/tc-2016-123, 2016.

Yashayev, I., and Loder, J. W.: Recurrent replenishment of Labrador Sea water and associated decadal-scale variability. J. Geophys. Res., 8095-8114, doi:10.1002/2016JC012046, 2016.

Zunino, P., Lherminier, P., Mercier, H., Daniault, N., García-Ibáñez, M. I., and Pérez, F.: The GEOVIDE cruise in May–June 2014 reveals an intense Meridional Overturning Circulation over a cold and fresh subpolar North Atlantic. Biogeosciences, 14, 5323-5342, doi:10.5194/bg-14-5323-2017, 2017.

Figure captions

Figure 1. Map of the bins along B-AX01 (black), B-AX02 (red), G-AX02 (blue), and N-AX01 (green). A typical example of ship track is shown along B-AX02.
Figure 2. B-AX01 (left) and B-AX02 (right) Hoevmøller diagrams of deviations from an average seasonal cycle. Salinity (top with vertical lines indicative of the crossing), temperature (middle), density (bottom). The sketch on top/left corner indicates where the lines are located with relation to main currents (red NAC and extensions, purple fresher slope and shelf currents.
Figure 3. G-AX01 (left) and N-AX02 (right) anomalies Hoevmøller diagrams of deviations from an average seasonal cycle. Salinity (top), temperature (middle), density (bottom) (see Fig. 1 for locations of sections). For salinity and density, different contours/color codes are used for G-AX01 and N-AX01.
Figure 4. Seasonal cycle of interannual RMS variability (left along B-AX01; right along B-AX02). S (top), T (middle) and density (bottom)
Figure 5. The principal components (PC) and spatial structure (EOF) of an empirical orthogonal function analysis of salinity jointly for B-AX01 and B-AX02 (07/1993-12/2017) (we applied a 15-month running mean prior to the EOF analysis). The PCs are normalized to variance 1, and the EOF are such that 1 indicates that the EOF explains 100% of total local variance.
Figure B.1. Comparison in 1993-2015 of S and T from B-AX01 with EN4 (blue) and CORA (red) gridded data (surface, full lines; 0-500m vertically integrated, dashed lines). Correlation coefficients are plotted, as well as the RMS standard deviations in the different products (the dashed black line is for B-AX01 data). The upper panels are for S, the lower panels for T.

Earth Syst. Sci. Data Discuss., https://doi.org/10.5194/essd-2018-22
Manuscript under review for journal Earth Syst. Sci. Data
Discussion started: 4 April 2018

Earth System Science Data Open Access Discussions

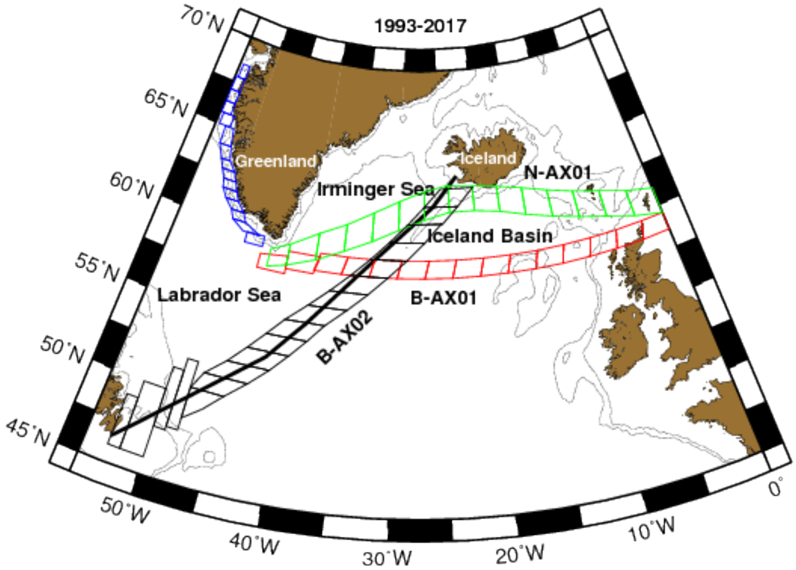

Figure 1. Map of the bins along B-AX01 (black), B-AX02 (red), G-AX02 (blue), and N-AX01 (green). A typical example of ship track is shown along B-AX02.

Earth Syst. Sci. Data Discuss., https://doi.org/10.5194/essd-2018-22
Manuscript under review for journal Earth Syst. Sci. Data
Discussion started: 4 April 2018

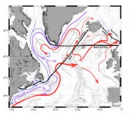

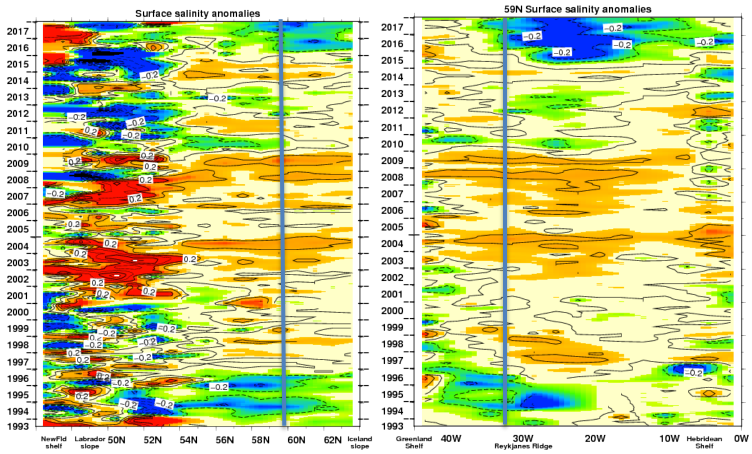

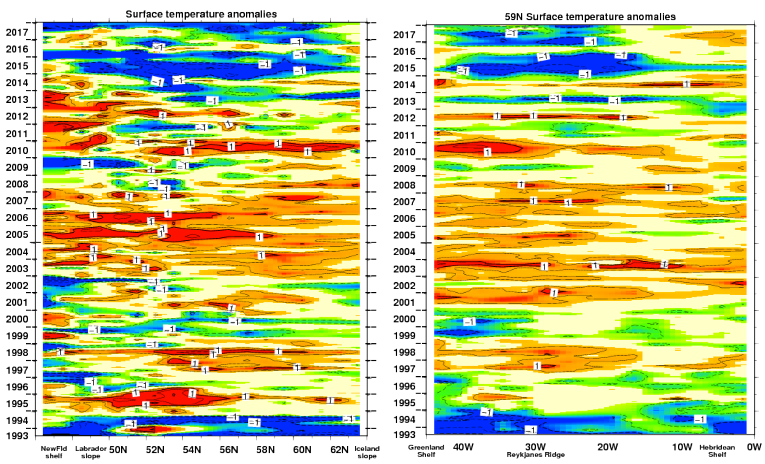

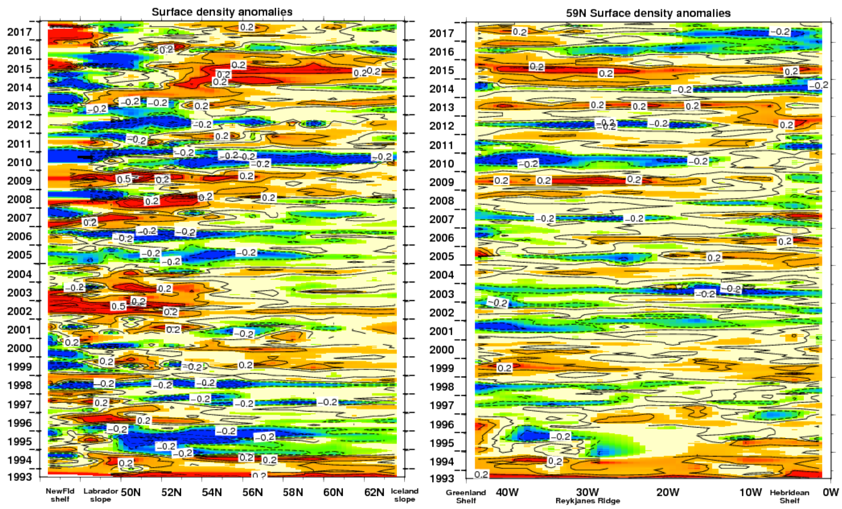

Figure 2. B-AX02 (left) and B-AX01 (right) Hoevmøller diagrams of deviations from an average seasonal cycle. Salinity (top with vertical lines indicative of the crossing), temperature (middle), density (bottom). The sketch on top/left corner indicates where the lines are located with relation to main currents (red NAC and extensions, purple fresher slope and shelf currents.

Earth Syst. Sci. Data Discuss., https://doi.org/10.5194/essd-2018-22
Manuscript under review for journal Earth Syst. Sci. Data
Discussion started: 4 April 2018

Open Access Earth System Science Data Discussions

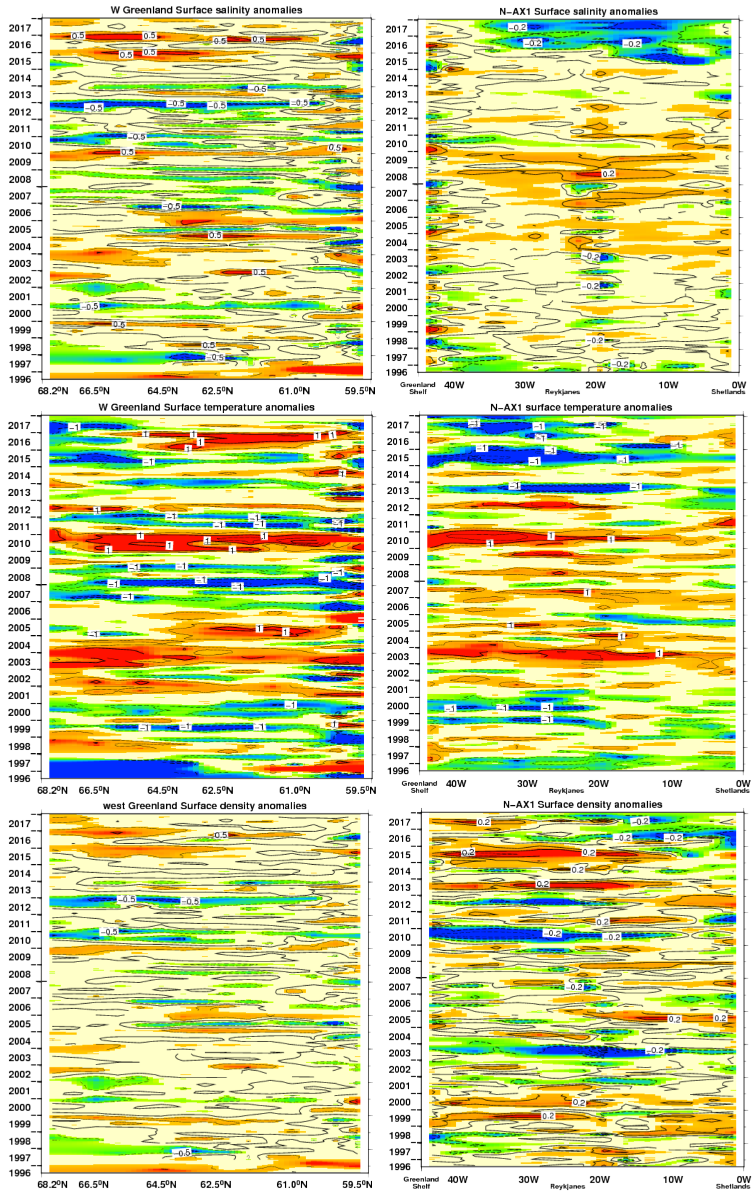

Figure 3. G-AX01 (left) and N-AXO1 (right) anomalies Hoevmøller diagrams of deviations from an average seasonal cycle. Salinity (top), temperature (middle),

Earth Syst. Sci. Data Discuss., https://doi.org/10.5194/essd-2018-22
Manuscript under review for journal Earth Syst. Sci. Data
Discussion started: 4 April 2018

density (bottom) (see Fig. 1 for locations of sections). For salinity and density, different contours/color codes are used for G-AX01 and N-AX01.

Open Access Earth System Science Data Discussions

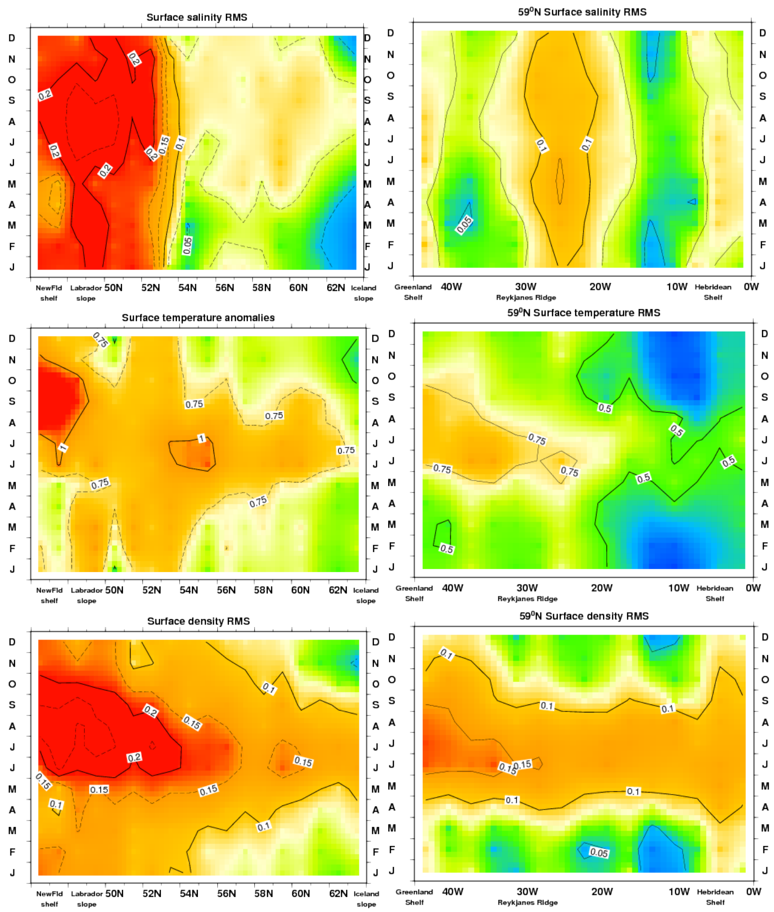

Figure 4. Seasonal cycle of interannual RMS variability (left along B-AX02; right along B-AX01). S (top), T (middle) and density (bottom)

Earth Syst. Sci. Data Discuss., https://doi.org/10.5194/essd-2018-22
Manuscript under review for journal Earth Syst. Sci. Data
Discussion started: 4 April 2018

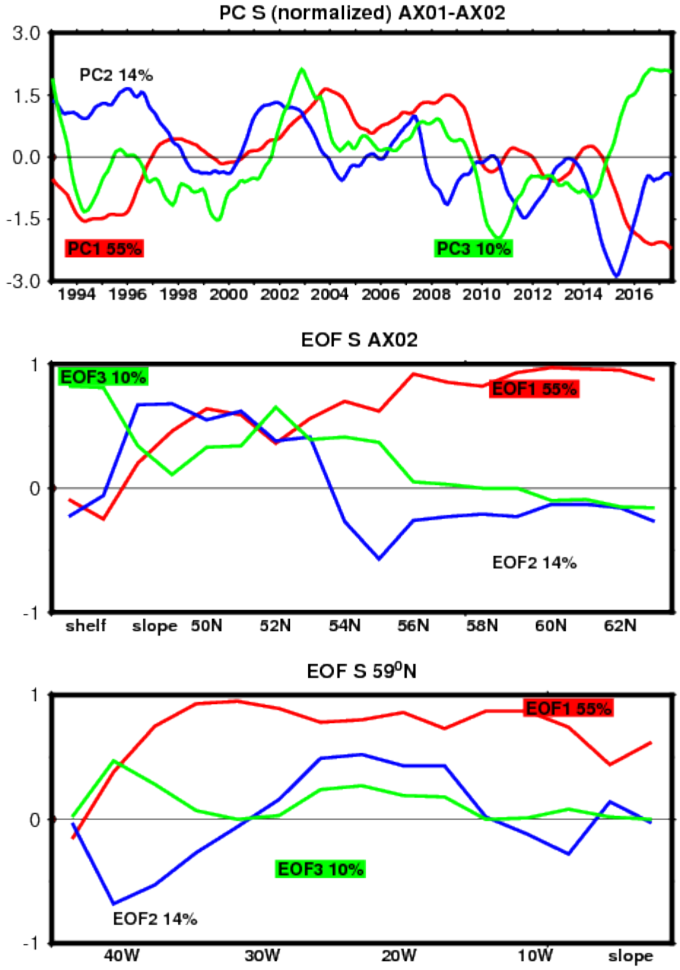

Figure 5. The principal components (PC) and spatial structure (EOF) of an EOF analysis of salinity jointly for B-AX01 and B-AX02 (07/1993-12/2017) (we applied a 15-month running mean prior to the EOF analysis). The PCs are normalized to variance 1, and the EOF are such that 1 indicates that the EOF explains 100% of total local variance.

Earth Syst. Sci. Data Discuss., https://doi.org/10.5194/essd-2018-22
Manuscript under review for journal Earth Syst. Sci. Data
Discussion started: 4 April 2018

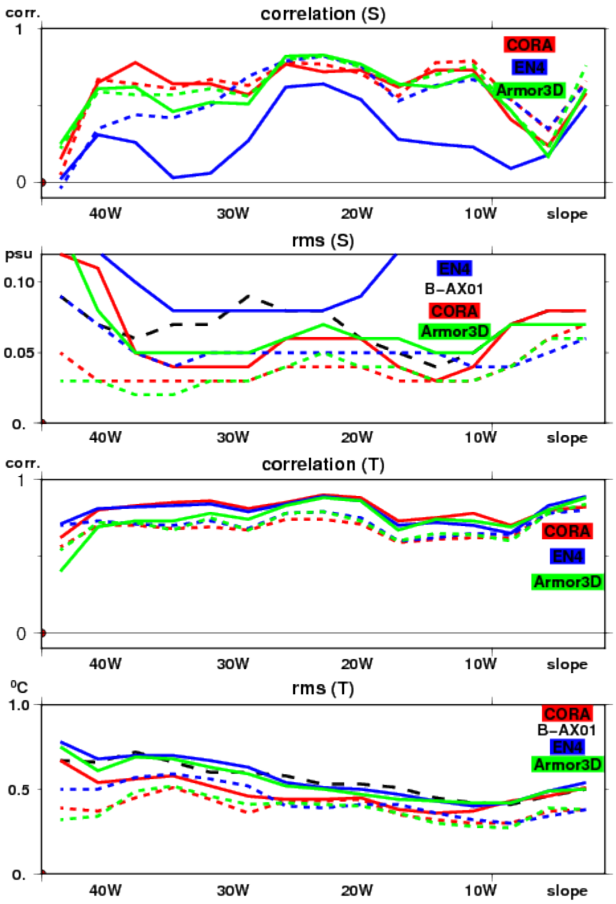

Figure B.1. Comparison in 1993-2015 of S and T from B-AX01 with EN4 (blue) and CORA (red) gridded data (surface, full lines; 0-500m vertically integrated, dashed lines). Correlation coefficients are plotted, as well as the RMS standard deviations in the different products (the dashed black line is for B-AX01 data). The upper panels are for S, the lower panels for T.